

## Pseudospark excited sub-THz frequency sources

H. Yin<sup>1</sup>, L. Zhang<sup>1</sup>, Y. Yin<sup>2</sup>, J. Zhao<sup>3</sup>, G. Shu<sup>1</sup>, W. He<sup>1</sup>, A. W. Cross<sup>1</sup>, A. D. R. Phelps<sup>1</sup>

<sup>1</sup>Department of Physics and SUPA, University of Strathclyde, Glasgow G4 0NG, Scotland, UK  
a.d.r.phelps@strath.ac.uk

<sup>2</sup>School of Physical Electronics, University of Electronic Science and Technology of China, Chengdu, 610054, China

<sup>3</sup>High Voltage Division, School of Electrical Engineering, Xi'an Jiaotong University, Xi'an, 710049, China

There are several advantageous features of using a pseudospark (PS) discharge [1] for electron beam production. One of these features is the formation of an ion channel following the pseudospark anode, which enables the beam to propagate and eliminates the need for a guiding magnetic field [2–5]. When a high voltage is applied to the hollow cathode, the electric field across the anode-cathode gap penetrates a short distance into the hollow cathode region due to the small cathode aperture. A PS discharge will occur if the pressure in the system is suitably low (typically 50–500 mTorr) so that the discharge is at the left-hand side (with respect to the minimum) of the Paschen curve. In such a PS discharge condition, the gas breakdown will occur along the longest possible path, allowing a virtual anode to form, extending from the anode into the hollow cathode region. As the virtual anode reaches the cathode surface field-enhanced emission begins to occur. Electrons begin emitting from the cathode surface at an increased rate, augmented by secondary emission and are accelerated toward the aperture by the electric field. Consequentially this rapid increase in electron emission results in a rapid increase in the beam current. As the beam propagates through the anode its front edge ionizes the background gas, forming a plasma channel, while the following beam electrons expel part of the plasma electrons so that an ion-channel is formed, confining the beam and eliminating the need for any external magnetic guide field. A high current density, high brightness electron beam with a sweeping voltage can therefore be generated and propagated by ion channel focusing.

Pseudospark discharges have been explored for various important applications, especially high quality electron beam generation for microwave sources [2, 5, 6] and potential terahertz devices. High frequency sources above 100 GHz are very attractive for a wide range of research and technical applications, including molecular spectroscopy, bio-imaging and security screening. As the frequencies move into the sub-terahertz and terahertz region, the size of device reduces greatly. This brings a challenge with regard to device fabrication. Therefore a compact and simplified structure is desirable, with the pseudospark-sourced electron beam an ideal choice for high power, high frequency sources. This paper presents some experimental results of the electron beam current dependence on the gap separation of a single-gap pseudospark structure. At a certain gap separation, the relationship between the beam current and discharge voltage has been studied [2]. It is found that the electron beam only starts to occur when the charging voltage is above a certain value and increases with the increasing discharge voltage following two tendencies. Under the same discharge voltage, the configuration with the larger electrode gap separation

will generate higher electron beam current. Because the energy of the high brightness electrons in the beam produced by a pseudospark is relatively low post acceleration experiments on the hollow cathode beam have also been successfully carried out [4, 5].

X-ray emission studies and spatial visualization of the PS beams have been used to improve the characterisation of these beams [7, 8]. Several experiments have successfully produced mm-wave/sub-THz radiation [9, 10]. Zhao et al. [11, 12] have measured the dependence of the PS beam on the gap separation and the beam variability in a post-accelerated PS [13]. Kumar et al. [14] have carried out an analysis of how the PS geometrical factors affect the PS emission. These studies have provided increased insight for the designs of future sub-terahertz and terahertz sources driven by PS electron beams.

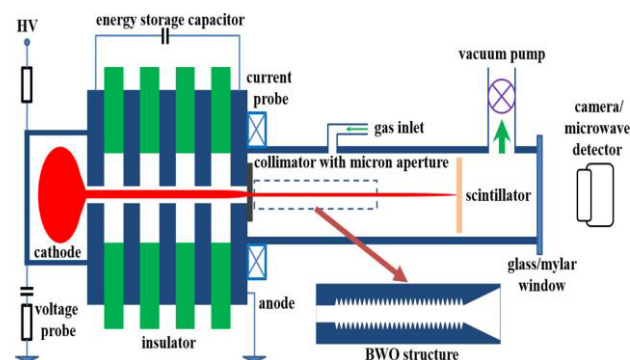


**Fig. 1.** Experimental configuration producing a micro-electron beam from a PS which is used to excite a 200 GHz BWO structure [9]

Fig. 1 shows the experimental configuration of a multigap PS discharge that produces a micro-electron beam. No magnetic field is needed to transport the electron beam. The rippled wall BWO structure is mounted immediately adjacent to the PS exit micro-aperture, so that the electron beam can pass through the BWO structure. The BWO structure, together with the conical radiation launching horn, was manufactured by high speed grinding of an aluminum former and the subsequent electrodeposition of a 5mm thick layer of copper on the aluminium former, which was later dissolved away in an alkali solution.

An electron beam ~1mm diameter carrying a current of up to 10A and current density of  $10^8 \text{ Am}^{-2}$ , with a sweeping voltage of 42 to 25 kV and pulse duration of 25 ns, was generated from the PS discharge. Fig. 2 shows the repeatable time-correlated electron beam voltage, the discharge current and the millimetre wave pulse. The electron beam current has a step of about 5A at the hollow cathode discharge phase and then a peak current of

about 10A follows in the conductive phase. The microwave radiation was mainly generated near this first 5 A step, because the correlated beam voltage has stronger coupling with the BWO structure. In the conductive phase, the beam voltage is too small to have efficient beam-wave interaction.

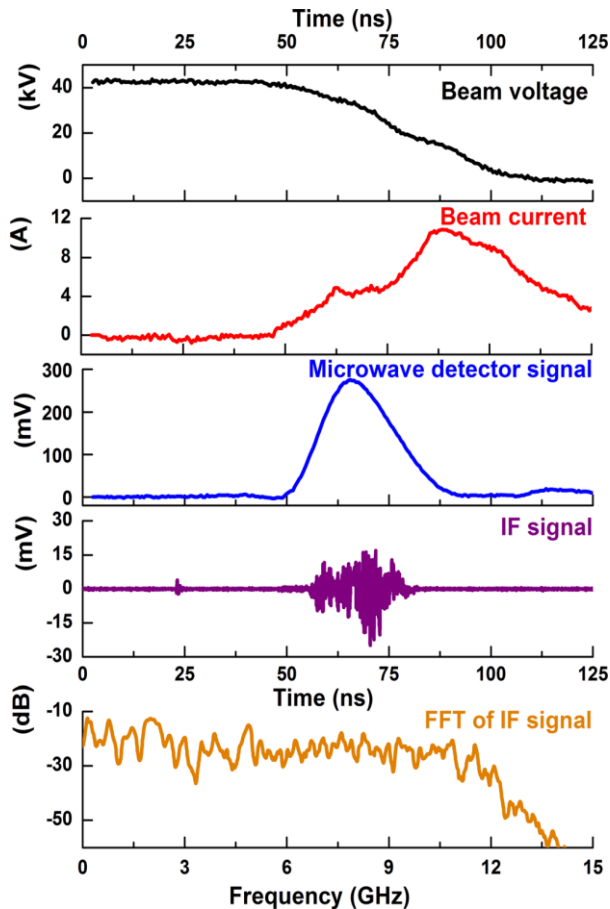


**Fig. 2.** Time-correlated electron beam voltage, current pulse, the radiation pulse from the 200 GHz BWO, the IF output from a harmonic mixer recorded on a deep memory (20 GHz) single shot digital storage oscilloscope, and FFT result of the intermediate frequency output [9]

The output power was measured using the general antenna theorem with the total power from a launching antenna, calculated by integrating its radiated power density over space. The integration was completed by numerically integrating the normalized mode profile of the launching horn and multiplying by the measured maximum power density. The result of this measurement was that the total power of the BWO in this frequency range was found to be 20 W.

#### Acknowledgements

The UK Engineering and Physical Research Council (EPSRC) is thanked for supporting this research. David Barclay provided valuable technical assistance.

#### References

1. Christiansen, J., and Schultheiss, C. Production of high current particle beams by low pressure spark discharges // *Zeitschrift für Physik A Atoms and Nuclei*. 1979. V. 290. No. 1. P. 35-41.
2. Yin, H., Robb, G.R.M., He, W., Phelps, A.D.R., Cross, A.W. and Ronald, K. Pseudospark-based electron beam and Cherenkov maser experiments // *Phys. Plasmas*. 2000. V. 7. No. 12. P. 5195-5205.
3. Yin, H., He, W., Cross, A.W., Phelps, A.D.R., and Ronald, K. Single-gap pseudospark discharge experiments // *J. Appl. Phys.* 2001. V. 90. No. 7. P. 3212-3218.
4. Yin, H., Cross, A.W., Phelps, A.D.R., Zhu, D., He, W., and Ronald, K. Propagation and post-acceleration of a pseudospark-sourced electron beam // *J. Appl. Phys.* 2002. V. 91. No. 8. P. 5419-5422.
5. Yin, H., Cross, A.W., He, W., Phelps, A.D.R., and Ronald, K. Pseudospark experiments: Cherenkov interaction and electron beam post-acceleration // *IEEE Trans. Plasma Sci.* 2004. V. 32. No. 1. P. 233-239.
6. Yin, H., Cross, A.W., He, W., Phelps, A.D.R., Ronald, K., Bowes, D., and Robertson, C.W. Millimeter wave generation from a pseudospark-sourced electron beam // *Phys. of Plasmas*. 2009. V. 16. No. 6. P. 063105.
7. Bowes, D., Yin, H., He, W., Zhang, L., Cross, A.W., Ronald, K., Phelps, A.D.R., Chen, D., Zhang, P., Chen, X., and Li, D. X-ray emission as a diagnostic from pseudospark-sourced electron beams // *Nuclear Instruments & Methods in Physics Research Section B-Beam Interactions with Materials and Atoms*. 2014. V. 335. No. P. 74-77.
8. Bowes, D., Yin, H.L., He, W.L., Ronald, K., Phelps, A.D.R., Chen, D.F., Zhang, P., Chen, X.D., Li, D.H., and Cross, A.W. Visualization of a Pseudospark-Sourced Electron Beam // *IEEE Trans. Plasma Sci.* 2014. V. 42. No. 10. P. 2826-2827.
9. He, W., Zhang, L., Bowes, D., Yin, H., Ronald, K., Phelps, A.D.R., and Cross, A.W. Generation of broadband terahertz radiation using a backward wave oscillator and pseudospark-sourced electron beam // *Appl. Phys. Lett.* 2015. V. 107. No. 13. P. 4.
10. Shu, G.X., He, W.L., Zhang, L., Yin, H.B., Zhao, J.P., Cross, A.W., and Phelps, A.D.R. Study of a 0.2-THz Extended Interaction Oscillator Driven by a Pseudospark-Sourced Sheet Electron Beam // *IEEE Trans. Electron Devices*. 2016. V. 63. No. 12. P. 4955-4960.
11. Zhao, J., Yin, H., Zhang, L., Shu, G., He, W., Zhang, J., Zhang, Q., Phelps, A.D.R., and Cross, A.W. Influence of the electrode gap separation on the pseudospark-sourced electron beam generation // *Phys. Plasmas*. 2016. V. 23. No. 7. P. 6.
12. Zhao, J., Yin, H., Zhang, L., Shu, G., He, W., Phelps, A.D.R., Cross, A.W., Pang, L., and Zhang, Q. Study of the beam profile and position instability of a post-accelerated pseudospark-sourced electron beam // *Phys. Plasmas*. 2017. V. 24. No. 3.
13. Zhao, J., Yin, H., Zhang, L., Shu, G., He, W., Zhang, Q., Phelps, A. D. R., and Cross, A. W. Advanced post-acceleration methodology for pseudospark-sourced electron beam // *Phys. Plasmas*. 2017. V. 24. No. 2.
14. Kumar, N., Pal, D.K., Lamba, R.P., Pal, U.N., and Prakash, R. Analysis of Geometrical Design Parameters for High-Energy and High-Current-Density Pseudospark-Sourced Electron Beam Emission // *IEEE Trans. Electron Devices*. 2017. V. 64. No. 6. P. 2688 - 2693.